Apelin, a potent diuretic neuropeptide counteracting vasopressin actions through inhibition of vasopressin neuron activity and vasopressin release

Nadia De Mota*†, Annabelle Reaux-Le Goazigo*†, Said El Messari*†, Nicolas Chartrel‡, Darren Roesch*, Cynthia Dujardin‡, Claude Kordon§, Hubert Vaudry‡, Françoise Moos¶, and Catherine Llorens-Cortes*‖

*Institut National de la Santé et de la Recherche Médicale, Unité 36, Collège de France, 75231 Paris, France; ‡Institut National de la Santé et de la Recherche Médicale, Unité 413, Université de Rouen, 76821 Mont-Saint-Aignan, France; §Institut Necker, 75015 Paris, France; and ¶Centre National de la Recherche Scientifique, Unité Mixte de Recherche 5101, 34094 Montpellier, France

Apelin, a recently isolated neuropeptide that is expressed in the supraoptic and the paraventricular nuclei, acts on specific receptors located on vasopressinergic neurons. The increased phasic pattern of these neurons facilitates sustained antidiuresis during dehydration or lactation. Here, we investigated whether apelin interacts with arginine vasopressin (AVP) to maintain body fluid homeostasis. We first characterized the predominant molecular forms of endogenous hypothalamic and plasma apelin as corresponding to apelin 13 and, to a lesser extent, to apelin 17. We then demonstrated that, in lactating rats, apelin was colocalized with AVP in supraoptic nucleus magnocellular neurons and given intracerebroventricularly inhibited the phasic electrical activity of AVP neurons. In lactating mice, intracerebroventricular administration of apelin 17 reduced plasma AVP levels and increased diuresis. Moreover, water deprivation, which increases systemic AVP release and causes depletion of hypothalamic AVP stores, decreased plasma apelin concentrations and induced hypothalamic accumulation of the peptide, indicating that AVP and apelin are conversely regulated to facilitate systemic AVP release and suppress diuresis. Opposite effects of AVP and apelin are likely to occur at the hypothalamic level through autocrine modulation of the phasic electrical activity of AVP neurons. Altogether, these data demonstrate that apelin acts as a potent diuretic neuropeptide counteracting AVP actions through inhibition of AVP neuron activity and AVP release. The coexistence of apelin and AVP in magnocellular neurons, their opposite biological effects, and regulation are likely to play a key role for maintaining body fluid homeostasis.

Apelin is a bioactive peptide recently isolated from bovine stomach extracts (1). It was identified as the endogenous ligand of the human orphan G protein-coupled receptor APJ (1, 2), reported to act as a coreceptor of CD4 for human and simian immunodeficiency viruses (3, 4). Apelin is a 36-aa peptide derived from a 77-aa precursor, preproapelin, for which cDNAs have been cloned from humans, cattle, rats, and mice (1, 5, 6). The apelin precursor has a fully conserved C-terminal sequence between Trp-55 to Phe-77, including the C-terminal 17 (Lys-Phe-Arg-Arg-Gln-Arg-Pro-Arg-Leu-Ser-His-Lys-Gly-Pro-Met-Pro-Phe; K17F) and 13 (Gln-Arg-Pro-Arg-Leu-Ser-His-Lys-Gly-Pro-Met-Pro-Phe; Q13F) amino acid sequences. These molecular species, and the pyroglutamyl form of Q13F (pE13F), exhibit the highest activities on extracellular acidification rate (1) and strongly inhibit forskolin-stimulated cAMP production in Chinese hamster ovary (CHO) cells expressing the human (5, 7, 8) or the rat (9) apelin receptor. These peptides also are highly potent inducers of rat apelin receptor internalization (10, 11).

In situ hybridization and RT-PCR studies have shown that the apelin precursor and apelin receptor mRNAs are expressed in various rat brain structures (6, 8, 9, 12, 13). Apelin-immunoreactive (IR) neurons are particularly abundant in hypothalamic nuclei, i.e., the supraoptic (SON), paraventricular (PVN), and arcuate nuclei (10, 14). High densities of apelin nerve fibers and terminals also

have been visualized in the SON, the PVN, the internal layer of the median eminence (14, 15), and the posterior pituitary (15). These observations suggest that apelin-containing cell bodies of the SON and PVN, like arginine vasopressin (AVP)- and oxytocin (OXY)-containing magnocellular neurons, project toward the neural lobe of the pituitary. These two neurohormones are released from nerve endings of the posterior pituitary into the systemic circulation and control fluid balance and milk ejection/uterus contractility (16). Indeed, Brailoiu *et al.* (15) reported that apelin IR colocalizes with neurophysin-I in a population of SON and PVN magnocellular neurons, indicating that apelin is expressed by OXY neurons. By inference, apelin-positive but OXY-negative neurons are likely to be vasopressinergic.

We previously have demonstrated that apelin receptors are expressed in magnocellular AVP neurons (10), an observation confirmed by another group (17). This finding suggests the possible involvement of apelin in the regulation of AVP release and body fluid homeostasis, as substantiated by physiological experiments showing that intracerebroventricular (i.c.v.) injection of apelin inhibits basal or dehydration-induced release of AVP as well as dehydration-induced water intake (6, 10, 18). These data support the contention that the close localization of apelin, apelin receptors, and AVP neurons is physiologically relevant. The role of apelin, however, in modulating AVP neuron activity and release, the regulation of its expression under physiological conditions known to activate AVP neurons, and the subsequent biological responses have not been analyzed so far.

The aim of the present study was first to identify, in the hypothalamus and the plasma, the molecular forms of apelin produced *in vivo*. Then, we determined in lactating animals whether apelin colocalized with AVP in magnocellular neurons, impaired their phasic electrical activity, modified systemic AVP release, and affected diuresis. We also investigated whether hypothalamic and plasma concentrations of apelin and AVP were affected by water deprivation to delineate how both peptides cooperate to maintain body fluid homeostasis.

Materials and Methods

Drugs and Antibodies. Apelin fragments were synthesized by Neosystem (Strasbourg, France). Human angiotensin (Ang) II and AngIII, AVP, and neuropeptide Y were purchased from Sigma. Rabbit polyclonal antibodies directed against the apelin fragment K17F were produced in the laboratory as described in ref. 10.

Guinea pig polyclonal AVP antibodies were purchased from Peninsula Laboratories and were used for immunohistochemistry as described in ref. 19.

Animals. We used adult rodents from Charles River Laboratories: male Sprague–Dawley or Wistar rats, female Sprague–Dawley rats (control or lactating, day 8 of lactation), or female Swiss mice (control or lactating, day 2 of lactation). The animals had free access to food and water, except in water-deprivation experiments in which animals were deprived of water for 24 or 48 h.

Iodinated Compounds. [^{125}I]pE13F [iodinated on Lys-8 by the Bolton–Hunter reagent; 2,000 Ci/mmol (1 Ci = 37 GBq)], used for RIA, was obtained from Amersham Pharmacia Biotech. [^{125}I]pE13F and [^{125}I]K17F (250 Ci/mmol), used to calibrate the Sephacryl S-100 column (Pharmacia Biotech), were iodinated on their single His residue by the chloramine T method as described in ref. 20.

Preparation of Tissue or Plasma Samples for RIA. Rats were decapitated and various brain regions and the pineal and the pituitary glands were dissected as described in ref. 21. Tissues were homogenized by sonication in 10–30 vol of cold 0.4 M $HClO_4$ containing 0.05% BSA. The homogenate was centrifuged at $17,000 \times g$ at 4°C for 20 min. The supernatant was collected, adjusted to pH 6.5, and centrifuged. The supernatant was mixed with 1 ml of 1% trifluoroacetic acid supplemented with 0.05% BSA and loaded onto a Sep-Pak C_{18} cartridge (Waters) equilibrated with 5 ml of 1% trifluoroacetic acid. The columns then were washed with 3 ml of 1% trifluoroacetic acid. Apelin peptides were eluted with 1.5 ml of 100% acetonitrile. The eluates were dried then redissolved in 0.25–0.5 ml of RIA buffer (19 mM $NaH_2PO_4 \cdot H_2O$/81 mM $Na_2HPO_4 \cdot 2H_2O$/50 mM NaCl/0.1% Triton X-100/0.01% NaN_3/0.1% BSA) and assayed. For plasma samples, trunk blood (4–5 ml) was collected in chilled tubes containing 0.25 ml of 0.3 M EDTA (pH 7.4) on ice and centrifuged at $1,600 \times g$ at 4°C for 15 min. Plasma (0.75 ml) was mixed with 0.1 ml of 0.5% BSA, and 0.25 ml of 3 M HCl was added before storage.

Preparation of Whole Rat Brain and Hypothalamic Extracts for Chromatographic Analysis. Ten whole brains (12 g wet weight) and 4,000 hypothalami (235 g wet weight) from adult rats were collected, boiled for 15 min in 0.5 M acetic acid, homogenized, and centrifuged at $6,000 \times g$ at 4°C for 30 min. The supernatants were removed and pumped at a flow rate of 1.5 ml/min through 2 Sep-Pak C_{18} cartridges connected in series for the pool of brains and through 10 Sep-Pak C_{18} cartridges in series for the pool of hypothalami. Bound material was eluted with acetonitrile:water:trifluoroacetic acid [60.0:39.9:0.1 (vol/vol/vol) for the pool of brains and 70.0:29.9:0.1 (vol/vol/vol) for the pool of hypothalami] and lyophilized.

Chromatographic Analysis of Rat Tissue Samples. The lyophilized extracts were resuspended in 1 M acetic acid and subjected to gel permeation chromatography on a 2.5×100-cm Sephacryl S-100 column equilibrated with 1 M acetic acid at a flow rate of 1.3 ml/min. Ninety eluting fractions (6.5 ml each) were collected every 5 min, dried, and assayed for apelin RIA or rat apelin receptor-enhanced GFP (EGFP) internalization. [^{125}I]AVP, [^{125}I]α-MSH, [^{125}I]pE13F, and [^{125}I]K17F, used as reference peptides, were chromatographed in the same conditions as tissue samples.

Apelin RIA Procedure. Samples were mixed with [^{125}I]pE13F (15,000 dpm) and K17F antiserum (1/10,000) to give a total volume of 0.2 ml and incubated at 4°C overnight. Then, 0.1 ml of 0.5% γ-globulin (Sigma) and 0.5 ml of 17% polyethylene glycol (Sigma) dissolved in 50 mM Tris·HCl buffer (pH 7.4) were added. The tubes were centrifuged at $2,200 \times g$ at 4°C for 20 min, and the radioactivity of the precipitates was measured.

AVP RIA Procedure. AVP concentrations were determined as described in refs. 22 and 23 from 0.2 ml of plasma by using a specific RIA kit (Peninsula Laboratories).

Internalization Assay and Confocal Microscopy. The internalization assay was performed on cycloheximide-treated CHO cells stably expressing the rat apelin-receptor-EGFP (9) cultured at a density of 2×10^5 cells per well as described in ref. 24. Cells were incubated in the presence or absence of pE13F or R10F or individual rat hypothalamic (5 μl) or plasma (45 μl) fractions were diluted in complemented Earle's buffer in a final volume of 50 μl. Internalization was examined with a Leica TCS SP 2 confocal laser scanning microscope (Leica Microsystems, Heidelberg), and quantification of apelin receptor-EGFP internalization was performed as described in ref. 24.

Tissue Preparation for Immunocytochemistry. Because Sprague–Dawley rats exhibit a higher concentration of apelin in the hypothalamus (18.0 ± 4.9 pmol/g of tissue) as compared to Wistar Kyoto rats (3.2 ± 0.7 pmol/g of tissue), pretreatment with colchicine previously used in Wistar Kyoto rats (10, 14) was not necessary to visualize apelin-positive neurons in female Sprague–Dawley rats.

Animals (control or lactating) were anesthetized with sodium pentobarbital (50 mg/kg, i.p.) and fixed by transcardiac perfusion of 4% paraformaldehyde in 0.1 M phosphate buffer (pH 7.4). Brains were postfixed in 4% paraformaldehyde (for 3 h) and cryoprotected by immersion for 24 h in 30% sucrose at 4°C. Brains were frozen in liquid nitrogen (-35°C), cut into coronal sections (20-μm thick) on a cryostat (Leica, Nussloch, Germany) at -20°C, and mounted on gelatin-coated glass slides.

Simultaneous Detection of Apelin and AVP Peptides by Double Immunofluorescence Staining. Sections were washed in PBS (pH 7.4), permeabilized with 0.5% Triton X-100 in PBS for 30 min, and incubated with 1% H_2O_2 in PBS for 30 min. Sections were incubated in a blocking solution consisting of 3% normal goat serum (Sigma) in PBS for 1 h. They then were incubated simultaneously with a rabbit polyclonal antibody against K17F (1:2,000) and a polyclonal guinea pig antibody against AVP (1:2,000) for 48 h at 4°C. Primary antibody binding was detected by incubation with Alexa 488-labeled goat anti-rabbit antibody (1:2,000) and Cy3-labeled donkey anti-guinea pig antibody (1:2,000) as secondary antibodies (Molecular Probes). The sections were observed under a confocal microscope (described above). The acquisition of pictures showing the apelin and AVP distributions in the same specimen were studied sequentially with excitation at 488 nm and 568 nm, respectively. Optical sections ($1,024 \times 1,024$) were taken by using a $\times$40 1.32 numerical aperture oil-immersion objective.

Electrophysiological Recordings. The procedure used for electrophysiological recordings was as described in ref. 25. AVP neurons were identified on the basis of their typical phasic pattern of activity (succession of periods of activity and silence), and K17F (4.3 ng = 2 pmol in 2 μl of cerebrospinal fluid-like medium) was injected into the third ventricle after 20 min of recording (control period).

Measurements of Diuresis, Natriuresis, and Kaliuresis in Conscious Lactating Mice. Diuresis, natriuresis, and kaliuresis were measured for 3 h after the i.c.v. injection of saline or K17F (2 μg) in lactating mice. After the i.c.v. injection, mice were placed in metabolic cages without pumps. Urine was collected, and its volume and urinary Na^+ and K^+ excretions were measured.

NEUROSCIENCE

Table 1. Crossreactivity of K17F antibodies with various apelin and bioactive peptides

Peptide	Sequence	Crossreactivity, %
K17F	Lys-Phe-Arg-Arg-Gln-Arg-Pro-Arg-Leu-Ser-His-Lys-Gly-Pro-Met-Pro-Phe	214
pE13F	pGlu-Arg-Pro-Arg-Leu-Ser-His-Lys-Gly-Pro-Met-Pro-Phe	100
R12F	Arg-Pro-Arg-Leu-Ser-His-Lys-Gly-Pro-Met-Pro-Phe	110
P11F	Pro-Arg-Leu-Ser-His-Lys-Gly-Pro-Met-Pro-Phe	48.2
R10F	Arg-Leu-Ser-His-Lys-Gly-Pro-Met-Pro-Phe	33.8
G5F	Gly-Pro-Met-Pro-Phe	26.7
K16P	Lys-Phe-Arg-Arg-Gln-Arg-Pro-Arg-Leu-Ser-His-Lys-Gly-Pro-Met-Pro	< 0.3
K15M	Lys-Phe-Arg-Arg-Gln-Arg-Pro-Arg-Leu-Ser-His-Lys-Gly-Pro-Met	< 0.3
AngII		1.1 ± 0.2
AngIII		0.9 ± 0.1
AVP		< 0.03
NPY		< 0.3

Crossreactivity of the binding of pE13F peptide to K17F antibodies with various apelin fragments and peptides determined by RIA, calculated as the percentage of binding of the apelin-related peptides referred to that of pE13F (100%). Values are expressed as means ($\pm$ SEM) of multiple assays ($n \geq 3$). NPY, neuropeptide Y.

Results

Characterization of the K17F Antiserum. Mean IC_{50} values for binding inhibition of [^{125}I]pE13F to the apelin antiserum was 0.28 ± 0.08 nM (data not shown). Minimal concentration of pE13F necessary to significantly displace the tracer was 6 fmol. Crossreactivity of the apelin antiserum with various N- and C-terminally truncated fragments of K17F and several other bioactive peptides is shown in Table 1. Taking reactivity with pE13F as 100%, the rank order of reactivity was K17F > pE13F = L36F ≈ R12F > P11F > R10F > G5F ≫ K16P = K15M, with negligible reactivity observed for AngII, AngIII, neuropeptide Y, and AVP (Table 1). Serial dilutions of tissue extracts and plasma samples gradually inhibited binding of [^{125}I]pE13F to the antiserum, and inhibition curves paralleled that of pE13F used as a standard (data not shown).

Distribution of Apelin IR in Various Rat Brain Regions, Pituitary and Pineal Glands, and Plasma. Large differences in apelin IR levels were observed in the six brain regions tested (Fig. 1A). Apelin levels were highest in the hypothalamus and lowest in the cerebellar and cerebral cortices. In both the pineal and the pituitary glands, apelin levels were 17 times higher than in the hypothalamus. High apelin concentration (3.8 pmol/ml) was detected in the plasma (Fig. 1A).

Characterization of Apelin-Related Peptides in Rat Brain, Hypothalamus, and Plasma Samples. Characterization of apelin-IR peptides was carried out by combining gel permeation chromatography with RIA detection and internalization assays. In hypothalamic extracts, a single component responsible for apelin-like IR was eluted in fractions 34 to 37 (Fig. 1B). Calibration of the Sephacryl S-100 column with neuropeptides of various molecular masses suggested that the IR peptide detected in the hypothalamus had a molecular mass (M) of ≈1,400–1,600 Da, within the range of that of pE13F (M = 1,534 Da) (Fig. 1B). Five-microliters of fractions 35, 36, and 37 promoted internalization of the rat apelin receptor-EGFP stably expressed in CHO cells (Fig. 2). Comparison of the intensity of internalization of the rat apelin receptor-EGFP observed in the presence of the active fractions those obtained with graded concentrations of synthetic pE13F (data not shown) revealed that the initial concentration of pE13F in fractions 35, 36, and 37 was ≈100 nM. Concurrently, estimation of pE13F concentration in these fractions, deduced from the value obtained by RIA, was 200 nM (Fig. 1B). In whole-brain extracts (data not shown) and in plasma samples (Fig. 1C), apelin-like IR eluted as two IR peaks, one in fraction 22 and the other around fraction 27, that exhibited the same retention times as [^{125}I]K17F and [^{125}I]pE13F, respectively (Fig. 1C). Applied on CHO cells stably expressing the rat apelin receptor-EGFP, fractions 26 and 27 were the most potent inducers of internalization of the rat apelin receptor (data not shown).

Colocalization of Apelin and AVP in SON Magnocellular Neurons. Within the hypothalamus, immunostaining for apelin was observed in the SON and PVN in control female rats (data not shown) and in the SON in lactating rats (Fig. 3A). Confocal microscopy analysis of coronal brain sections simultaneously labeled with antisera directed against K17F and AVP revealed that most of the SON magnocellular neurons displaying AVP IR also were immunolabeled for apelin in the SON of female control (data not shown) and lactating rats (Fig. 3 C and F). However, apelin IR also was observed in neurons that were negative for AVP (Fig. 3C), probably OXY neurons. A dense fiber network of SON magnocellular neurons also was double-labeled. At a higher magnification, many vesicles, IR for both apelin and AVP, were visualized within the somata and processes (Fig. 3F, large arrow). In some double-labeled perikarya, three distinct vesicles IR for apelin, AVP, or both peptides were observed (Fig. 3F, arrowhead). Similarly, the hypothalamo-neurohyphophyseal tracts of SON and PVN AVP neurons projecting in the internal zone of the median eminence also contained apelin (Fig. 3 G–I). At a higher magnification, many fibers of this network were immunostained for apelin, AVP, or both peptides (Fig. 3I Inset).

Electrical Activity of SON AVP Neurons After Intraventricular Injection of K17F in Lactating Rats. Because during lactation AVP neurons are more sensitive to hydric challenges (26), the study was performed on lactating rats to better differentiate AVP from OXY neurons. AVP neurons typically display phasic activity (succession of periods of activity, or "bursts of spikes," and silences) (27, 28). During lactation, this phasic pattern is reinforced, and the activation of AVP neurons leads to higher mean values of the activity quotient (Q) (percentage of time spent by the neuron in activity) than are observed in male rats (0.55 ± 0.06 vs. 0.35 ± 0.06 in males, $P < 0.05$, $n = 23$ and 26 neurons, respectively). Furthermore, for 60% of the neurons, Q values were between 0.4 and 0.8 in lactating rats, and between 0 and 0.4 in male rats. The response to acute i.c.v. injection of K17F (4.3 ng or 2 pmol) was tested on eight neurons displaying the typical firing pattern of AVP neurons. K17F induced gradual and sustained inhibition (up to 60 min after injection) of the phasic pattern in all neurons tested (Fig. 4), as shown by decreased intraburst spike frequency from 5.7 ± 0.9 spikes per s during the control period to 4.8 ± 1.0 spikes per s ($P < 0.05$, Student's paired t test) and burst duration (from 28 ± 9 s in controls to 16 ± 5 s, $P < 0.05$). In contrast, the duration of silences increased from 20 ± 6 s to 28 ± 7 s ($P < 0.05$). Changes in the phasic pattern resulted in a significant decrease in activity quotient Q (from 0.61 ± 0.10 to 0.44 ± 0.10, $P < 0.01$).

Apelin and AVP Levels in the Hypothalamus and Plasma After Water Deprivation. After 24 and 48 h of water deprivation, hypothalamic apelin levels increased by 167% and 81%, respectively ($2.62 \pm$
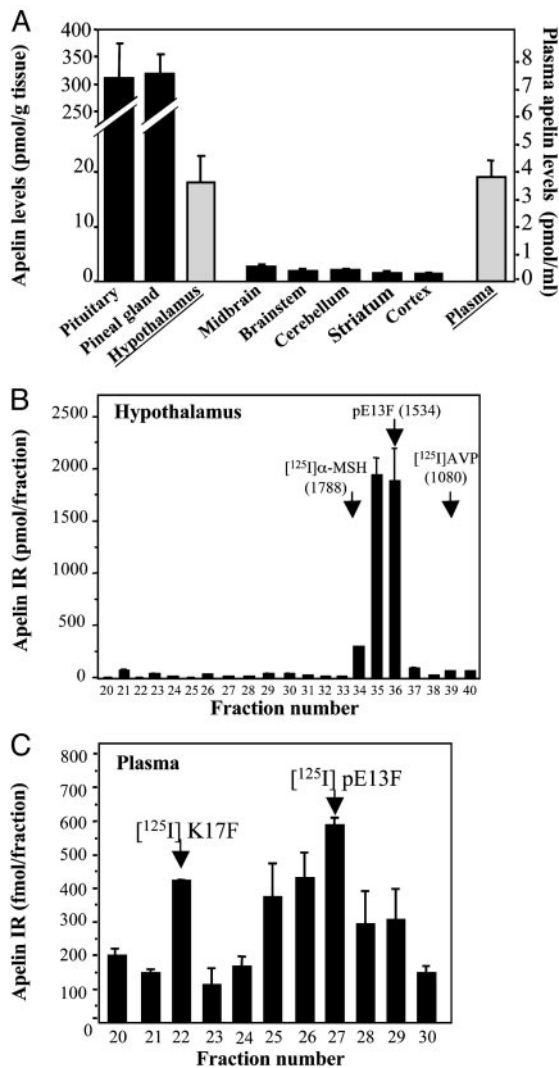
Fig. 1. Distribution and characterization of apelin-related peptides in rat brain, pituitary gland, pineal gland, and plasma. (*A*) Apelin IR levels were quantified by RIA. Results are expressed in pmol/g of tissue or pmol/ml of plasma as the mean ± SEM of at least six independent experiments. (*B* and *C*) Apelin IR detected in gel permeation chromatography for fractions 20–40 of rat hypothalamic extracts (*B*) or fractions 20–30 of rat plasma (*C*). Results are expressed as the mean ± SEM of three independent experiments.

Fig. 2. Effects of partially purified rat hypothalamic fractions on the internalization of the rat apelin receptor-EGFP. Confocal images of rat apelin receptor-EGFP CHO cells. Before ligand exposure (T_0) or in presence of the inactive apelin fragment R10F (100 nM), the apelin receptor is confined to the plasma membrane. Internalization of the apelin receptor occurs in presence of pE13F (100 nM) or the rat hypothalamic fractions 35, 36, or 37.

0.28 and 1.78 ± 0.20 vs. 0.98 ± 0.08 pmol per hypothalamus in controls), and plasma apelin levels significantly decreased by 34% and 70%, respectively (2.30 ± 0.31 and 1.06 ± 0.32 vs. 3.46 ± 0.25 pmol/ml in controls) (Fig. 5). In contrast, hypothalamic AVP levels decreased by 46% after 48 h of water deprivation (10.5 ± 1.1 in dehydrated rats vs. 19.5 ± 2.3 pmol per hypothalamus in controls, $P < 0.05$), whereas after 24 and 48 h of dehydration, plasma AVP levels significantly increased by 160% (16.9 ± 3.9 fmol/ml) and 130% (15.0 ± 1.1 fmol/ml), as compared to controls (6.5 ± 1.7 fmol/ml) (Fig. 5). The correlation between apelin accumulation (1.64 pmol) in the hypothalamus and decreased plasma levels (1.16 pmol/ml) after 24 h of water deprivation strongly suggests that circulating apelin originates at least in part from magnocellular neurons.

Central Effects of K17F on Systemic AVP Release, Diuresis, Natriuresis, and Kaliuresis in Conscious Lactating Mice. Lactating mice exhibited higher plasma AVP levels than did control female mice (41.5 ± 4.1 in lactating mice vs. 15.1 ± 1.5 pg/ml in controls, $P < 0.01$). i.c.v.
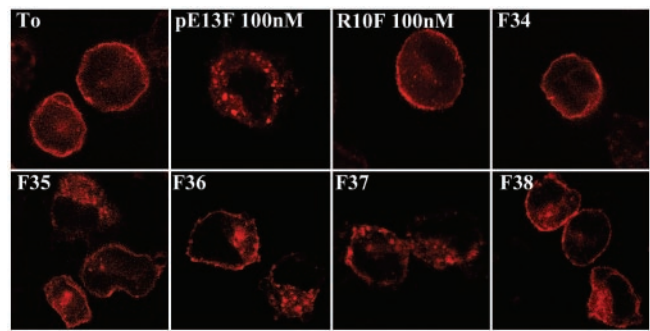
injection of K17F in lactating mice (2 μg or 0.93 nmol per animal) significantly decreased plasma AVP levels by 40% (25.3 ± 3.3 pg/ml) as compared with lactating controls injected with saline (41.5 ± 4.1 pg/ml, $P < 0.01$) (Fig. 6*A*). In the electrophysiological experiments described above, lactating rats receiving i.c.v. injections of K17F displayed much higher diuresis than did those injected with saline (data not shown). This finding led us to investigate the possible effects of K17F on diuresis, natriuresis, and kaliuresis in conscious lactating mice. i.c.v. injection of K17F (2 μg or 0.93 nmol per animal) resulted in a significantly higher diuresis (5.55 ± 0.77 μl of urine/min) than was observed in lactating mice injected with saline (1.83 ± 0.33 μl of urine/min) (Fig. 6*B*). The maximum concentrations of Na^+ and K^+ in the urine were significantly lower in mice treated with K17F than in controls (70 ± 10 mmol/l vs. 221 ± 54 mmol/l, $P < 0.05$) (Fig. 6*C*). In mice treated i.c.v. with K17F, however, urinary excretion of Na^+ ($U_{Na}V = 0.51 ± 0.14$ μmol/min) and K^+ ($U_KV = 0.51 ± 0.08$ μmol/min) did not differ significantly from that in control mice ($U_{Na}V = 0.41 ± 0.09$ μmol/min; $U_KV = 0.38 ± 0.03$ μmol/min) (Fig. 6*D*).

Discussion

The recently isolated neuropeptide apelin acts on specific receptors expressed in rat hypothalamic nuclei involved in the control of body fluid homeostasis and neuroendocrine regulation (6, 9, 10, 17). Concurrently, high densities of apelin neurons have been visualized in the rat hypothalamus, especially in the SON, PVN, and arcuate nucleus (10, 14). By using a highly selective antibody against K17F, we detected large amounts of apelin IR in the hypothalamus and the pituitary gland, substantiating previous reports showing high levels of preproapelin mRNA in these structures (5, 6, 8, 12, 13). High apelin IR also was recovered from the plasma. To define the molecular forms of apelin produced *in vivo*, we combined separation by gel permeation chromatography and RIA detection and identified pE13F and, to a lesser extent, K17F as the predominant forms of apelin present in the whole brain, hypothalamus, and plasma. This finding contrasts with the molecular forms previously recovered from testis and uterus, corresponding to molecular weights close to that of apelin 36, whereas in the mammary gland, apelin peptides with molecular weights similar to those of pE13F and apelin 36 were described (29). We also demonstrated that the IR material extracted from the hypothalamus and plasma corresponds to bioactive apelin and not to inactive degradation products, because it recognized the rat apelin receptor and induced its internalization.

In the hypothalamus, apelin recently was reported to colocalize with OXY in magnocellular neurons (15). By inference, apelin-positive but OXY-negative neurons can be assumed to contain
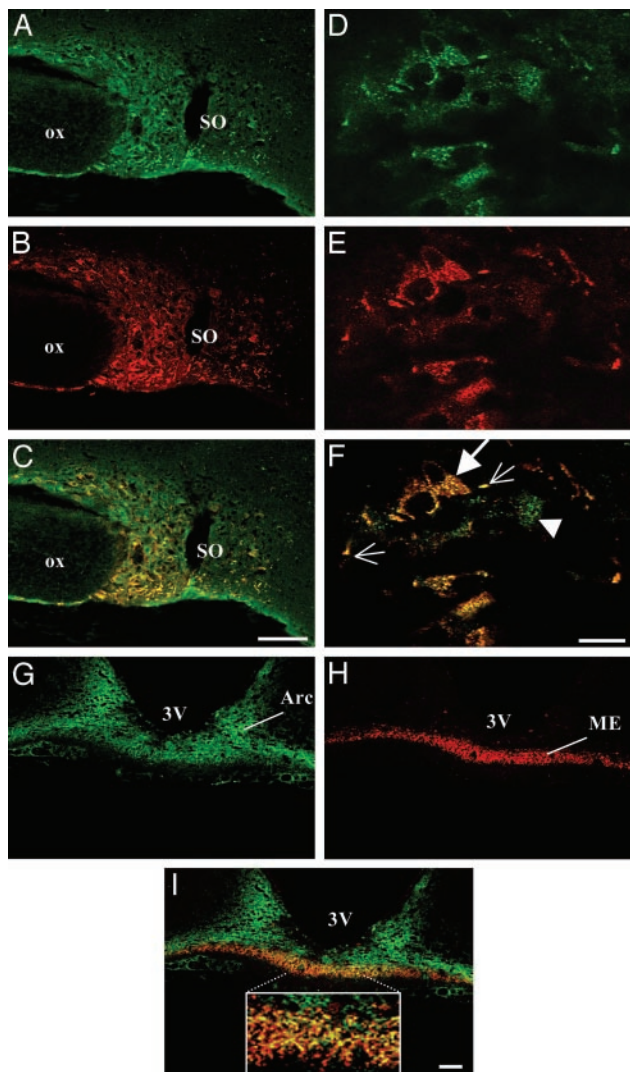
Fig. 4. Electrical activity of AVP neurons in the SON of anesthetized lactating rats after central injection of K17F. The discontinuous display of firing rate (spikes per s) of a single AVP neuron shown here clearly illustrates the progressive installation and persistence of an inhibitory effect induced by injection of K17F (2 pmol) into the third ventricle.

thus tested, in lactating rats, the effect of apelin on the electrical activity of AVP SON neurons exhibiting a reinforced phasic pattern during lactation. The infusion of a low concentration of K17F into the third ventricle inhibited the phasic firing activity of these neurons, thereby decreasing AVP release from neurohypophyseal axon terminals, as substantiated by the decrease in plasma AVP levels after i.c.v. injection of K17F in lactating mice. In agreement with this observation, a marked decrease in systemic AVP release has been reported after i.c.v. injection of K17F or pE13F in control or water-deprived animals (10). Altogether, these data suggest that apelin is likely released from AVP cell bodies to inhibit both AVP neuron activity and release by means of a direct action on the apelin autoreceptors expressed by AVP/apelin-containing neurons.

We further investigated whether endogenous apelin, like AVP, is affected by dehydration. A 24 or 48 h water-deprivation period

Fig. 3. Confocal images of magnocellular neurons double-labeled with antisera against apelin and AVP in lactating rats. (*A–C*) Low-magnification views of the SON, showing the colocalization of apelin (green) (*A*) and AVP (red) (*B*). (*D–F*) High magnification views of the SON showing the colocalization (*F*) of apelin (*D*) with AVP (*E*) in cytoplasmic vesicles within the cell bodies (large arrow) and neuronal processes (small arrows). Some SON neurons (arrowhead) contain three distinct types of vesicles labeled for apelin, AVP, or both peptides (*F*). (*G–I*) Low-magnification views of the arcuate nucleus (Arc) and the internal zone of the median eminence (ME) that also contain apelin. (*I Inset*, internal zone) At higher magnification, many fibers were immunostained for apelin, AVP, or both peptides. In *C, F,* and *I*, yellow staining shows the colocalization of apelin and AVP. 3V, third ventricle; OX, optic chiasma. (Scale bar = 50 μm in *A–C* and *G–I* and 10 μm in *D–F*).

AVP. Here we show that, in lactating rats characterized by increases in both synthesis (30) and release of AVP and OXY (26, 31), many SON and PVN magnocellular neurons IR for AVP did indeed also contain apelin. Thus, AVP neurons express apelin, in addition to apelin receptors (10, 17) and V1a and V1b vasopressinergic receptors (19), suggesting a direct autocrine feedback regulation of these neurons by the two neuropeptides.

In response to osmotic stimulation, an increased somatodendritic release of AVP from SON and PVN cell bodies occurs (32, 33), enhancing by means of V1 autoreceptors the phasic activity pattern of AVP neurons (32) and thereby facilitating systemic AVP release. In a similar way, apelin may be involved in autocrine somatodendritic feedback regulation of neurohypophyseal AVP neurons. We
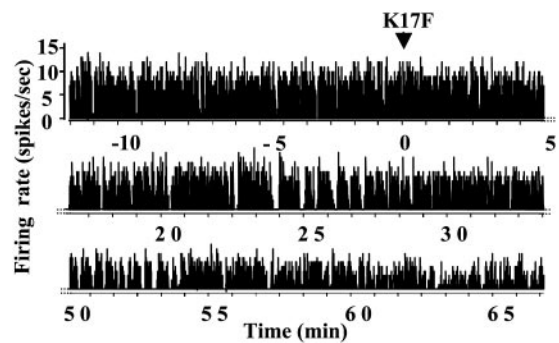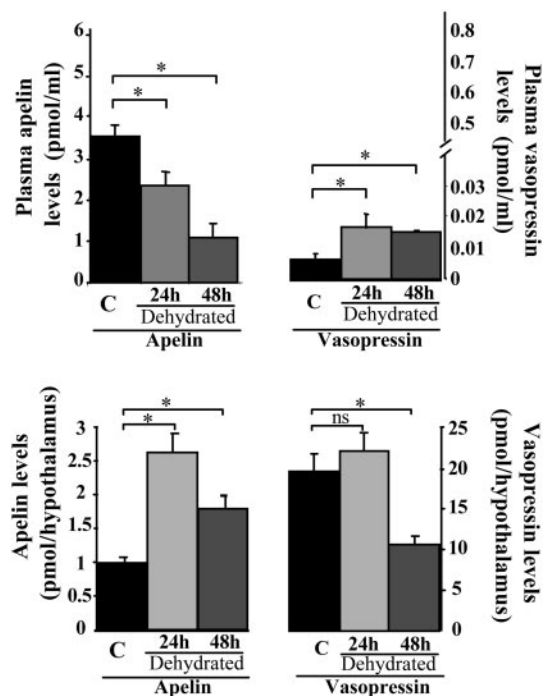

Fig. 5. Modification of plasma and hypothalamic apelin and AVP levels after water deprivation. Rats were deprived of water for 24 h (*n* = 10) or 48 h (*n* = 10). Plasma and hypothalamic apelin and AVP IR levels were measured by RIA. Mean ± SEM of six independent experiments carried out in duplicate.
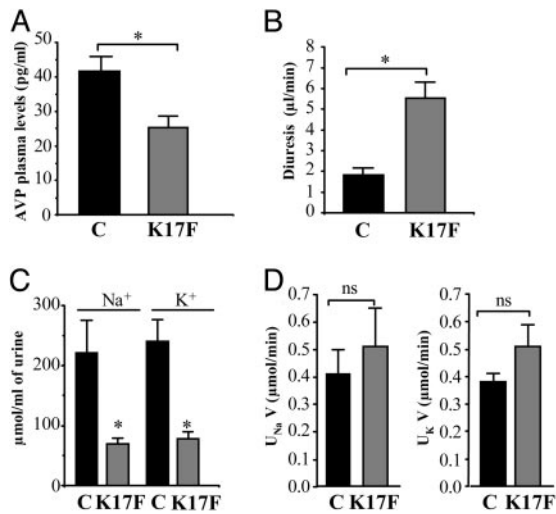
Fig. 6. Effects of i.c.v. injection of K17F on systemic AVP release, diuresis, natriuresis, and kaliuresis in conscious lactating mice. (*A*) Systemic AVP release was estimated by measuring plasma AVP levels by RIA after the i.c.v. injection of saline or K17F (0.93 nmol = 2 μg) in lactating mice. (*B–D*) Diuresis (*B*), urinary concentrations of Na^+ and K^+ (*C*), and Na^+ and K^+ excretion rates ($U_{Na}V$ and U_KV) (*D*) were measured for 3 h after the i.c.v. injection of saline or K17F (2 μg). Mean ± SEM, $n = 5$ in each group. *, $P < 0.05$ vs. control; ns, no significant difference vs. control animals.

resulted in a large increase in hypothalamic apelin levels that was mirrored by decreased plasma apelin levels, suggesting that, under these conditions, the peptide accumulated within hypothalamic neurons instead of being released. Apelin response to dehydration is thus opposite to that of AVP, which is released faster than it is synthesized, resulting in depletion of AVP hypothalamic stores (34). Opposite responses of apelin and AVP occurring during water deprivation also are consistent with the observation that in some magnocellular neurons, distinct vesicles are IR for apelin, AVP, or both peptides, as previously reported for galanin and AVP (35). Magnocellular AVP neurons also are known to express leu-enkephalin and dynorphin (36). As AVP, these peptides are depleted after osmotic stimulation, whereas the levels of the corresponding mRNAs are increased (36). Apelin thus appears to be the

only peptide colocalized with AVP that exhibits an opposite regulation during water deprivation. This reverse regulation reflects opposite mechanisms of action of the two peptides. During dehydration, while the increased somatodendritic release of AVP (33) will optimize phasic activity, facilitating systemic AVP release (ref. 32 and see references therein), apelin accumulates in SON and PVN neurons, instead of being systemically and probably intranuclearly released. Thus, decreased local supply of apelin to SON and PVN AVP cell bodies may facilitate the expression by AVP neurons of an optimized phasic activity, by lowering the inhibitory action of apelin on these neurons.

Antagonistic regulation of both peptides is physiologically relevant for maintaining body fluid homeostasis because, by this way, AVP and apelin act in concert to facilitate systemic AVP release and avoid additional water loss at the kidney level. This fine-tuning regulation is required as both peptides have opposite biological effects: AVP has pressor activity (37), whereas apelin is hypotensive (6, 10, 38); AVP acts as an antidiuretic (37), whereas we show here that apelin has a diuretic effect in conscious lactating animals, without affecting natriuresis and kaliuresis.

In conclusion, we have demonstrated that, in lactating animals, the recently identified neuropeptide apelin colocalizes with AVP in magnocellular neurosecretory neurons and inhibits the typical phasic firing pattern of these neurons, thereby resulting in decreased systemic AVP release and increased diuresis. In addition, after water deprivation, endogenous levels of both peptides are conversely regulated and thus reinforce systemic AVP release necessary for a sustained antidiuresis. These findings highlight the crucial role played by apelin in the maintenance of body fluid homeostasis by counteracting AVP actions.

Note Added in Proof. After this paper was submitted for publication, an immunohistochemical study performed in the laboratory of A. Beaudet using our polyclonal antibody directed against apelin showed that after dehydration the number of magnocellular apelin-immunoreactive cells increased significantly, whereas that of AVP-immunoreactive neurons significantly decreased (39), in agreement with our data on the opposite regulation between apelin and vasopressin.

1. Tatemoto, K., Hosoya, M., Habata, Y., Fujii, R., Kakegawa, T., Zou, M. X., Kawamata, Y., Fukusumi, S., Hinuma, S., Kitada, C., *et al.* (1998) *Biochem. Biophys. Res. Commun.* **251,** 471–476.
2. O'Dowd, B. F., Heiber, M., Chan, A., Heng, H. H., Tsui, L. C., Kennedy, J. L., Shi, X., Petronis, A., George, S. R. & Nguyen, T. (1993) *Gene* **136,** 355–360.
3. Rucker, J., Edinger, A. L., Sharron, M., Samson, M., Lee, B., Berson, J. F., Yi, Y., Margulies, B., Collman, R. G., Doranz, B. J., *et al.* (1997) *J. Virol.* **71,** 8999–9007.
4. Edinger, A. L., Hoffman, T. L., Sharron, M., Lee, B., Yi, Y., Choe, W., Kolson, D. L., Mitrovic, B., Zhou, Y., Faulds, D., *et al.* (1998) *J. Virol.* **72,** 7934–7940.
5. Habata, Y., Fujii, R., Hosoya, M., Fukusumi, S., Kawamata, Y., Hinuma, S., Kitada, C., Nishizawa, N., Murosaki, S., Kurokawa, T., *et al.* (1999) *Biochim. Biophys. Acta.* **13,** 25–35.
6. Lee, D. K., Cheng, R., Nguyen, T., Fan, T., Kariyawasam, A. P., Liu, Y., Osmond, D. H., George, S. R. & O'Dowd, B. F. (2000) *J. Neurochem.* **74,** 34–41.
7. Zou, M. X., Liu, H. Y., Haraguchi, Y., Soda, Y., Tatemoto, K. & Hoshino, H. (2000) *FEBS Lett.* **473,** 15–18.
8. Medhurst, A. D., Jennings, C. A., Robbins, M. J., Davis, R. P., Ellis, C., Winborn, K. Y., Lawrie, K. W., Hervieu, G., Riley, G., Bolaky, J. E., *et al.* (2003) *J. Neurochem.* **84,** 1162–1172.
9. De Mota, N., Lenkei, Z. & Llorens-Cortes, C. (2000) *Neuroendocrinology* **72,** 400–407.
10. Reaux, A., De Mota, N., Skultetyova, I., Lenkei, Z., El Messari, S., Gallatz, K., Corvol, P., Palkovits, M. & Llorens-Cortes, C. (2001) *J. Neurochem.* **77,** 1085–1096.
11. Zhou, N., Fan, X., Mukhtar, M., Fang, J., Patel, C. A., Dubois, G. C. & Pomerantz, R. J. (2003) *Virology* **307,** 22–36.
12. Hosoya, M., Kawamata, Y., Fukusumi, S., Fujii, R., Habata, Y., Hinuma, S., Kitada, C., Honda, S., Kurokawa, T., Onda, H., *et al.* (2000) *J. Biol. Chem.* **275,** 21061–21067.
13. O'Carroll, A. M., Selby, T. L., Palkovits, M. & Lolait, S. J. (2000) *Biochim. Biophys. Acta.* **21,** 72–80.
14. Reaux, A., Gallatz, K., Palkovits, M. & Llorens-Cortes, C. (2002) *Neuroscience* **113,** 653–662.
15. Brailoiu, G. C., Dun, S. L., Yang, J., Ohsawa, M., Chang, J. K. & Dun, N. J. (2002) *Neurosci. Lett.* **327,** 193–197.
16. Brownstein, M. J., Russell, J. T. & Gainer, H. (1980) *Science* **207,** 373–378.
17. O'Carroll, A. M. & Lolait, S. J. (2003) *J. Neuroendocrinol.* **15,** 661–666.
18. Taheri, S., Murphy, K., Cohen, M., Sujkovic, E., Kennedy, A., Dhillo, W., Dakin, C., Sajedi, A., Ghatei, M. & Bloom, S. (2002) *Biochem. Biophys. Res. Commun.* **291,** 1208–1212.
19. Hurbin, A., Boissin-Agasse, L., Orcel, H., Rabie, A., Joux, N., Desarmenien, M. G., Richard, P. & Moos, F. C. (1998) *Endocrinology* **139,** 4701–4707.
20. Tonon, M. C., Burlet, A., Lauber, M., Cuet, P., Jegou, S., Gouteux, L., Ling, N. & Vaudry, H. (1985) *Neuroendocrinology* **40,** 109–119.
21. Glowinski, J. & Iversen, L. L. (1966) *J. Neurochem.* **13,** 655–669.
22. Reaux, A., Fournie-Zaluski, M. C., David, C., Zini, S., Roques, B. P., Corvol, P. & Llorens-Cortes, C. (1999) *Proc. Natl. Acad. Sci. USA* **96,** 13415–13420.
23. Zini, S., Fournie-Zaluski, M. C., Chauvel, E., Roques, B. P., Corvol, P. & Llorens-Cortes, C. (1996) *Proc. Natl. Acad. Sci. USA* **93,** 11968–11973.
24. Lenkei, Z., Beaudet, A., Chartrel, N., De Mota, N., Irinopoulou, T., Braun, B., Vaudry, H. & Llorens-Cortes, C. (2000) *J. Histochem. Cytochem.* **48,** 1553–1564.
25. Belin, V. & Moos, F. (1986) *J. Physiol.* **377,** 369–390.
26. Poulain, D. A., Wakerley, J. B. & Dyball, R. E. (1977) *Proc. R. Soc. London B* **196,** 367–384.
27. Dutton, A. & Dyball, R. E. (1979) *J. Physiol. (London)* **290,** 433–440.
28. Bicknell, R. J. & Leng, G. (1981) *Neuroendocrinology* **33,** 295–299.
29. Kawamata, Y., Habata, Y., Fukusumi, S., Hosoya, M., Fujii, R., Hinuma, S., Nishizawa, N., Kitada, C., Onda, H., Nishimura, O. & Fujino, M. (2001) *Biochim. Biophys. Acta.* **23,** 2–3.
30. Mahata, S. K., Mahata, M., Hortnag, H., Fischer-Colbrie, R., Steiner, H. J., Dietze, O. & Winkler, H. (1993) *J. Neuroendocrinol.* **5,** 323–330.
31. Gimpl, G. & Fahrenholz, F. (2001) *Physiol. Rev.* **81,** 629–683.
32. Gouzenes, L., Desarmenien, M. G., Hussy, N., Richard, P. & Moos, F. C. (1998) *J. Neurosci.* **18,** 1879–1885.
33. Ludwig, M. (1998) *J. Neuroendocrinol.* **10,** 881–895.
34. Zingg, H. H., Lefebvre, D. & Almazan, G. (1986) *J. Biol. Chem.* **261,** 12956–12959.
35. Landry, M., Vila-Porcile, E., Hokfelt, T. & Calas, A. (2003) *Eur. J. Neurosci.* **17,** 579–589.
36. Meister, B., Cortes, R., Villar, M. J., Schalling, M. & Hökfelt, T. (1990) *Cell Tissue Res.* **260,** 279–297.
37. Manning, M., Lowbridge, J., Haldar, J. & Sawyer, W. H. (1977) *Fed. Proc.* **36,** 1848–1852.
38. Tatemoto, K., Takayama, K., Zou, M. X., Kumaki, I., Zhang, W., Kumano, K. & Fujimiya, M. (2001) *Regul. Pept.* **99,** 87–92.
39. Reaux-Le Goazigo, A., Morinville, A., Burlet, A., Llorens-Cortes, C. & Beaudet, A. (May 24, 2004) *Endocrinology*, 10.1210/en.2004-0384.

NEUROSCIENCE